



ELSEVIER

Available online at www.sciencedirect.com**ScienceDirect**

Procedia Engineering 88 (2014) 208 – 215

**Procedia
Engineering**www.elsevier.com/locate/procedia

International Symposium on Dynamic Response and Failure of Composite Materials, DRaF2014

Ballistic performance of multi-layered fabric composite plates impacted by different 7.62 mm calibre projectiles

A. Manes ^{a*}, L.M. Bresciani ^a, M. Giglio ^a^a Politecnico di Milano - Dipartimento di Meccanica, Via La Masa 1, 20156 Milano,

Abstract

At present, the use of refined numerical simulation is gaining more and more importance, especially in extreme load cases where large experimental test programmes are not feasible. A validated numerical methodology can be exploited to investigate critical behaviour as a “virtual test”. According to this premise, a numerical investigation is presented in this work to study the ballistic resistance of Kevlar29-Epoxy fabric plates subjected to impacts of small calibre projectiles, armour piercing (AP), ball type, and a blunt shaped projectile (BSP), all with a 7.62 mm diameter. The numerical models were developed using the explicit finite element code LS - DYNA. The composite plate is 5 mm thick, made up of 12 layers. The fabric is impregnated in Epoxy matrix, to guarantee both structural and ballistic resistance, and is a 2D plain-weave. The mechanical properties of the projectiles’ deformable materials were modelled by means of the Johnson-Cook plasticity model, which also includes the failure criterion. The composite plate is modelled using a mixed Macro-homogenous / Meso-heterogeneous approach. In particular, the area around the impact adopts the Meso-heterogeneous modelling, in which the woven yarns and the matrix are separate parts able to interact, to increase the efficiency of the numerical methodology, allowing the modelling of the friction between the yarns, the delamination and the fibre-matrix debonding. This method needs to assign separately the mechanical properties to the fabric and the matrix as well as the damage criteria for the yarns, the matrix and the delamination. In the Macro-homogenous approach, which models the remainder of the composite plate, the yarns and the matrix are considered as a unique homogenous mean, to which equivalent orthotropic mechanical properties of the impregnated fabric are assigned. The numerical investigation mainly focuses on the residual velocity of the impacting projectiles, identifying the ballistic limit of each couple projectile-target.

© 2014 The Authors. Published by Elsevier Ltd. This is an open access article under the CC BY-NC-ND license (<http://creativecommons.org/licenses/by-nc-nd/3.0/>).

Peer-review under responsibility of the Organizing Committee of DRaF2014

Keywords: Numerical model, Composite, Blunt projectile, Armour piercing projectile, Ball projectile, LS-DYNA, Meso-scale.

* Corresponding author. Tel.: + 39 0223998630; fax: +39 02 23998263.

E-mail address: andrea.manes@polimi.it

1. Introduction

Numerical modelling by means of the Finite Element Method (FEM) is an efficient environment to reproduce a complex phenomenon since it allows choosing the phenomena to be simulated in a multiphysics environment. Creating a numerical model of ballistic impacts is not straightforward and requires the correct choice of several features. The choice of the length scale, together with the constitutive material models and the related parameters is a key point especially in the fields of composites, which are made of different materials. Several approaches have been used and developed during the last years and are reported in the literature. In particular, two different techniques of modelling have been employed in the literature, one technique does not reproduce all the yarns and the matrix but considers the layers as a unique homogenous mean, with equivalent orthotropic mechanical properties [1, 2, 3, 4, 5]. This approach most likely does not allow the detailed investigation of complex phenomena [1]. The *Meso-heterogeneous* model [1, 6, 7, 8], instead reproduces every single yarn and the epoxy matrix, as well as the interaction among these. This approach provides a more complete awareness of the phenomena and specifically of the damage features, as proven in the comparison with the homogeneous approach in [1]. In the present work, the numerical study of the ballistic resistance of Kevlar29-Epoxy fabric plates subjected to impacts of different 7.62 calibre projectiles is presented. The numerical models were developed using the explicit finite element code LS-DYNA®. The composite plate is 5 mm thick, made up of 12 layers. The fabric is impregnated in Epoxy matrix, to guarantee both structural and ballistic resistance, and is a 2D plain-weave, with no yarns woven among the layers, but with yarns woven alternatively among them, within every layer. The choice of evaluating the ballistic performance of the composite plate only by means of the numerical approach is justified by the broad exploitation of the numerical methodology in other impact models by the authors [1, 9, 10, 19], with excellent agreement with the experimental data.

1. Numerical model

All the simulations were run in LS-Dyna® and all the analysis adopted the explicit scheme formulation. The energy ratio criterion was adopted to evaluate the acceptability of the simulations: the criterion considers the total energy of the system that should remain constant during the impact. Hence, the ratio between total energy, initial total energy and work of the external forces should remain as close as possible to one, acceptable within 5%.

1.1. *Meso-heterogeneous model*

The approach is defined *Meso-heterogeneous* from [1] since the yarns and the matrix are reproduced individually. As mentioned above, this approach was already adopted in the literature [1, 6, 7, 8] but only in another work by the authors [1] the matrix is modelled, as it is in this work. The modelling of the matrix caused some difficulties, since the matrix surrounding the yarns has a complex geometry that would generate an unstable mesh, if not opportunely treated. The composite plate is not modelled in its entirety with the *Meso-heterogeneous* approach, because this would imply a very high computational cost. Therefore, the approach studied in [1, 6] in which every layer is divided into two zones (see Figure 1) was adopted. The primary yarns, which are those in direct contact with the projectile tips, and the yarns in the immediate vicinity of the impact area are reproduced with the *Meso-heterogeneous* approach, while the rest of the layer adopts the *Macro-homogenous* approach with shell elements[1]. The choice of reproducing the primary yarns in their entire length was made because these are the most stressed and deformed yarns in the impact zone, those which carry most of the load and are most severely damaged [11]. Alternatively, a square region could be reproduced around the impact area, but it would introduce a discontinuity along the primary yarns, giving poor results in the work of Rao et al [6]. The size of the cross *Meso-area*, for the one quarter symmetry model, is equal to 7.5 mm as adopted in [1], in which the projectile calibre was equal to 10 mm; this size was assessed and retained adequately wider than the projectile dimensions, therefore for the 7.62 calibre projectiles, 7.5 mm is furthermore suitable. The two different areas tied, using the routine TIED_NODE_TO_SURFACE that was adopted in [1].

1.2. Geometry reproduction

Starting from the geometry of the woven fibres, the dimensions of the yarns were measured by means of high resolutions pictures of the cross section of a composite plate, analysed with digital image software. The average measured dimension of the cross section of the yarns is about 1.2 mm in width and 0.25 mm in height; the thickness of a single layer is about 0.4 mm, this value was obtained from the datasheet of the manufacturer. The open-source software TexGen®, developed by the University of Nottingham [26], has been used to generate the computational geometry of the fabric, starting from simple properties: knowing the type of the fabric (2D plain weave), the thickness of the layer and the dimensions of the yarns, a composite base unit is generated. Afterwards, the geometries of the fabric and of the matrix surrounding it were exported to the numerical solver, where they were subjected to meshing and refinement. The final result is a structured mesh for both the yarns and the matrix, with hexahedral elements with one integration point (C3D8R), visible in Figure 1.

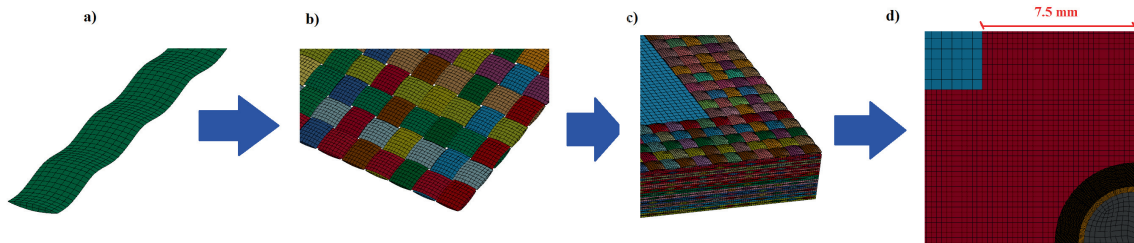


Figure 1: individual steps of the creation of the Meso-heterogeneous model: single yarn (a), woven fabric (b), multi-layer composite plate with matrix (c) and final assembly with the projectile pictured from the above (d)

1.3. Mechanical properties of the composite

The Meso-area needs the properties of the yarns and the matrix to be assigned individually: the stress-strain relationship of the matrix and the fibres is supposed to be perfectly-elastic until failure, this hypothesis is often used in composite modelling [12, 13]. The properties of Kevlar®29 and epoxy matrix [14] are reported in Table 1; the damage mode is implemented in the solver through the routine ADD_EROSION, imposing the equivalent threshold strain and the ultimate tensile strength (σ_{lf}) as the criterion of failure for both the yarns and the matrix.

Table 1: mechanical properties of the yarns and the matrix [14]

	Kevlar® 29	Epoxy resin
ρ $\left[\frac{Kg}{m^3} \right]$	1440	1300
E [Gpa]	83	2.8
G [Gpa]	29	1
ν	0.44	0.35
σ_f [MPa]	3620	83
ε_f [%]	4.4	3

The Macro-homogeneous area requires the assignment of the equivalent orthotropic mechanical properties of the woven fabric impregnated in the matrix. The routine adopted to reproduce the orthotropic mechanical properties is called MAT_ENHANCED_COMPOSITE_DAMAGE (054/055) [15], which also includes one failure criterion for the fibres and one for the matrix. The failure of the fibres is achieved under tensile stress (1) or compression (2):

$$e_f^2 = \left(\frac{\sigma_{11}}{X_t} \right)^2 + \beta \left(\frac{\sigma_{12}}{S_c} \right)^2 - 1 \begin{cases} \geq 0 & \text{failed} \\ < 0 & \text{elastic} \end{cases} \quad (1)$$

$$e_c^2 = \left(\frac{\sigma_{11}}{X_c}\right)^2 - 1 \begin{cases} \geq 0 & \text{failed} \\ < 0 & \text{elastic} \end{cases} \quad (2)$$

Where X_t and X_c are the longitudinal tensile and compressive strength and S_c is the shear strength. Imposing $\beta = 0$, the shear component is not taken into account and the criterion is found to be better comparable to experimental data [15]. The Tsai-Wu criterion [15] has the following formulation that represents the failure of the matrix under tension and compression (3):

$$e_{md}^2 = \frac{\sigma_{22}^2}{Y_c Y_t} + \left(\frac{\sigma_{12}}{S_c}\right)^2 + \frac{(Y_c - Y_t)\sigma_{22}}{Y_c Y_t} - 1 \begin{cases} \geq 0 & \text{failed} \\ < 0 & \text{elastic} \end{cases} \quad (3)$$

This criterion includes the compressive (Y_c) and tensile (Y_t) strength, and the in plane shear strength (S_c). The employed mechanical properties are reported in Table 2.

Table 2: Mechanical properties of plain-woven fabric Kevlar®29/epoxy [3, 4, 5, 16, 17]

ρ $\left[\frac{Kg}{m^3}\right]$	density	1440
E1 [Gpa]	Young modulus x	18.5
E2 [Gpa]	Young modulus y	18.5
E3 [Gpa]	Young modulus z	6
G12 [Gpa]	Shear modulus xy	0.77
G13, G23 [Gpa]	Shear modulus yz, xz	5.43
ν_{12}	Poisson coefficient	0.25
ν_{13}, ν_{23}	Poisson coefficient	0.33
X_t [MPa]	Longitudinal tensile strength x	1850
Y_{1t} [MPa]	Longitudinal tensile strength y	1850
X_c [MPa]	Longitudinal compressive strength x	185
Y_{1c} [MPa]	Longitudinal compressive strength y	185
S_c [Mpa]	Shear strength xy	77

1.4. Projectile features and mechanical properties

All the projectiles employed in the analyses have a calibre of 7.62 mm. The aim is to evaluate the ballistic performance of the composite plate against common ammunition. The selected projectiles include two Armour Piercing (AP) (ogival steel core AP and conical tungsten carbide core AP), one Ball and one blunt shape projectile (BSP) that is more commonly employed in research experimental tests. The BSP has a totally different shape, thus it involves a different perforation phenomenon, which is capable of perforating the target by shear plugging as shown in [1], and is thus interesting to be compared with the other ammunition types. The core and the jacket of the ogival 7.62 mm AP projectile are made of steel and copper, while the other conical AP projectile has a tungsten carbide penetrator with a conical tip shape, encapsulated in a brass (CuZn30) sabot. The Ball type projectile has a soft core (lead alloy) with a red brass (CuZn10) jacket. The BSP is made of pure tungsten (99.5%). The mass of each projectile is given by the manufacturers, except for the BSP projectile, to which the weight equal to 9.5 g (defining the length of the cylinder) was assigned, which is also the weight of the Ball projectile; the AP steel core projectile weighs 9.24 g and the AP tungsten carbide core projectile has a mass of 11.68 g.

The steel and tungsten cores are modelled as rigid materials, because of their high mechanical properties with respect to the other metals and the composite: this assumption is also made in [1, 10] with excellent results. Lead alloy, brass (CuZn30), red brass (CuZn10) and copper adopt the Johnson-Cook constitutive model; copper and brass

(CuZn30) adopt the J-C failure model, while lead and red brass (CuZn10) adopt a constant strain failure value, in accordance with experimental tests performed in [19, 20] on these materials. The ultimate strain of red brass is equal to 40% and for lead equal to 31%. These ultimate strain values were employed in preliminary analyses also in the compression region of the fracture triaxiality locus, but the Ball projectile was subjected to widespread anomalous erosion leading to the deletion of almost all of the elements of the projectile.

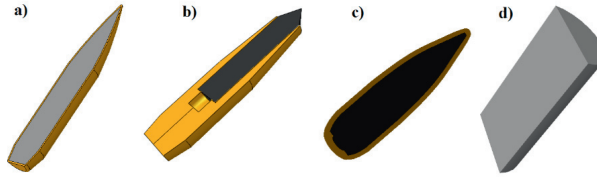


Figure 2: a) ogival AP steel core with copper jacket, b) AP conical tungsten carbide penetrator with a brass sabot, c) soft-core (lead) Ball projectile with a red brass jacket d) BSP projectile

Hence, after running other analyses without the possibility of eroding the elements, a maximum plastic strain equal to about 150% was measured at the tip of the projectile: it was then decided to introduce this threshold strain value in the compression region of the triaxiality fracture locus, since a ductile metal in compression is not well modelled by severe erosion of the majority of the elements, while in tension the experimental values were kept, with much less anomalous erosion and realistic results. The equation of state of the deformable materials is the Mie-Gruneisen. The parameters of the J-C constitutive and failure law [10, 19, 23] and of the Mie-Gruneisen equation of state [21, 22, 24, 25] are reported in Table 3 and 4.

Table 3: Johnson Cook constitutive and damage parameters [10, 19, 23]

Material	Constitutive model					Damage model				
	A [Mpa]	B [Mpa]	N	C	M	D1	D2	D3	D4	D5
Copper	89.63	291.64	0.31	0.025	1.09	0.54	4.88	3.03	0.014	1.12
Brass (CuZn30)	111.69	504.69	0.42	0.009	1.68	0.00	2.65	0.62	0.028	0.00
Red Brass (CuZn10)	90.0	628.03	0.702	0.265	1.68	/	/	/	/	/
Lead	1	55.551	0.098	0.230	1	/	/	/	/	/

Table 4: Mie-Gruneisen EOS parameters [21, 22, 24, 25]

Material	C [mm/s]	S1	Y0
Copper	8.960e+006	1.500	2.119
Brass (CUZn30)	3.834e+006	1.429	2.000
Red Brass(CuZn10)	3.834e+006	1.429	2.000
Lead	2.028e+006	1.627	2.253

1.5. Delamination and contact modelling

The contact between the projectile and the target is defined by means of the routine ERODING_SURFACE_TO_SURFACE [15], which is based on the penalty formulation. The target is made of a multi-layer structure and the layers are glued together by means of the epoxy matrix. This means that delamination occurs among them, and after that, layers are free to move and get in contact with each other. The embedded LS-Dyna® routine called AUTOMATIC_SURFACE_TO_SURFACE_TIEBREAK [15] has been employed. This approach requires normal and tangential threshold stresses; once these are reached separation between the surfaces in contact is allowed. In particular, the failure criterion is given by the following equation [15]:

$$f_{del} = \left(\frac{\sigma_n}{S_n}\right)^2 + \left(\frac{\tau}{S_s}\right)^2 - 1 \begin{cases} \geq 0, failure \\ < 0, no failure \end{cases} \quad (4)$$

Where σ_n and τ are the normal and tangential stresses calculated at every time step, S_n and S_s are the threshold stresses for failure, equivalent to 34.5 Mpa and 9 Mpa respectively [5]. This contact model is penalty based and after the failure of the tiebreak contact, it behaves like an erosion contact, so elements might be eroded. The contact modelling between the yarns and the matrix that are, as mentioned above, separate parts joint together until a force breaks the bond, is the same assuming that the connection breaks up when the failure criterion (6) is satisfied. The normal and tangential threshold stresses were hypothesized to be the same as the delamination since the connection between the layers can be considered to be similar to the connection between the matrix and a single yarn.

1.6. Friction modelling

Friction between the projectile and the target is considered null, as done in previous works [1, 3, 4], while friction among the yarns that can interact, moving one against the other under the forces introduced by the projectile, is reproduced. In [6] the static coefficient of friction μ_s and the dynamic friction coefficient μ_d were determined experimentally for Kevlar® yarns, the effective friction coefficient is modelled with the following law:

$$\mu = \mu_d + (\mu_s - \mu_d)e^{-\alpha|V_{rel}|} \quad (5)$$

Where V_{rel} is the relative velocity between the respective surfaces in contact and α is an exponential decay coefficient, characteristic of the transition from static to dynamic friction of the entities in contact. α is set equal to 10^8 , $\mu_s = 0.23$ and $\mu_d = 0.19$ [6]. In [18] it is shown that the ballistic limit has a strong dependency on the friction coefficient with values up to 0.1, while for higher values the ballistic limit reaches a horizontal asymptote; the above cited values are therefore in the zone of non-dependency of the ballistic limit from the friction coefficient.

2. Results

The main parameter of interest for this research is the residual velocity of the projectile after the impact against the composite target. The ballistic limit points out the efficiency of the composite plate in stopping different types of ammunition, with almost the same mass and overall diameter but different shape and material. Therefore, different simulations with all the projectiles were run at several impact velocities against the 5 mm thick Kevlar®29 and epoxy matrix, in order to determine the ballistic limit of every couple projectile-target, and also to understand the differences in the penetration capability of each ammunition. The ballistic limit was measured by determining the highest velocity at which complete perforation did not occur, with a 10 m/s gap between the impact velocities of the analyses close to the limit; this gap was chosen to minimize the high computational cost of the several analyses, with each analysis taking approximately three days to run.

Figure 3 shows the trends of the residual velocities of the various projectiles studied in this work. The comparison of the different curves shows that the BSP projectile has the highest ballistic limit, equal to 140 m/s, while the armour piercing (AP) projectiles have a higher perforation performance, with the ballistic limit equal to 90 m/s for the tungsten carbide core projectile and between 70 m/s and 80 m/s for the steel core ammunition. At 80 m/s, the steel core AP projectile perforates the target plate but remains stuck in the composite with zero residual velocity, and therefore, according to the definition, the ballistic limit is lower than this value. The tungsten core projectile shows a better perforation capability than the steel core projectile at high impact velocities, maybe also due to its greater mass, but the curve of the steel AP bends less rapidly as the velocity decreases to the ballistic limit, which in fact is lower for the steel core AP projectile. A similar behaviour is observed for the Ball projectile, which has a ballistic limit that lies between 90 m/s and 100 m/s, greater than the AP projectiles, but lower than the BSP ammunition. The Ball ammunition has an ogival shape similar to the AP steel projectile and for this reason, the curves of the AP steel and the Ball projectiles have a similar trend with a gentle bend.

This behaviour differs from the AP tungsten and the BSP ammunition, which are characterized by a less sharp

shape of their tips (the BSP is totally flat) and therefore lower local shear stresses. The tip of the lead core Ball projectile undergoes deformation and some erosion (see Figure 4.c), causing a loss in its perforation performance, compared to the AP steel projectile. At 110 m/s, also the Ball projectile is stuck in the composite plate, with complete perforation.

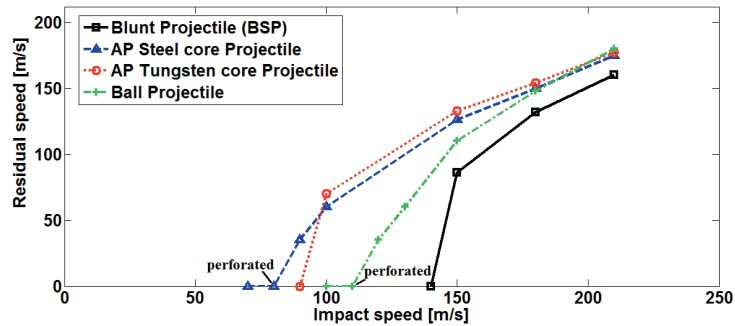


Figure 3: Residual velocities versus impact velocities for different projectiles against the 5 mm Kevlar®29-epoxy target

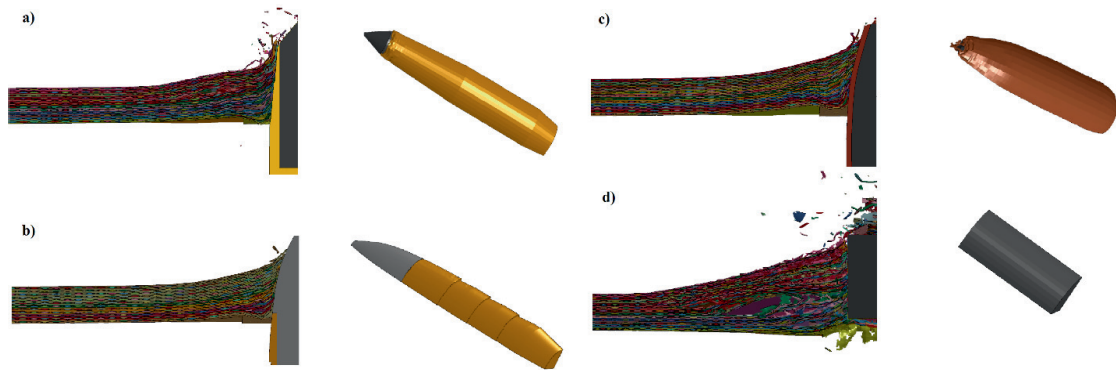


Figure 4: delamination comparison with impacts at 150 m/s and respective projectile deformations after the impact (right). a) AP conical tungsten carbide penetrator with deformed brass sabot, b) Ogival AP steel core with low deformation of the copper jacket, c) deformation of the soft-core (lead) Ball projectile with red brass jacket d) undeformed BSP projectile

As the impact velocity rises, up to over 200 m/s, all the residual velocities curves tend to a common asymptote, and the gap between the velocities of the BSP and the AP/Ball projectiles decreases. According to [1], at high impact speed the BSP projectile creates important shear plugging, resulting in its capability to perforate the target with almost the same performance as the AP and Ball projectiles. The analysis of the morphological features of projectiles and the target after the impact showed that the jackets of the AP projectiles do not undergo severe deformation and erosion, while this phenomenon takes place on the Ball projectile tip; in this case the jacket is deformed and eroded, with the lead core that gets in contact with the composite and in turn is damaged. Delamination is a common negative phenomenon in composite targets, which could lead to internal damages even if the projectile does not perforate the plate. Figure 4 shows a comparison of the sections of the composite plates impacted by the projectiles at 150 m/s. The BSP generates the most severe delamination along the layers, with a widespread radial delamination. The AP and the Ball projectiles cause much less delamination with damage and deformation of the composite plate concentrated around the projectile, overall the AP with a steel core and the lead core Ball ammunition, while the AP with tungsten carbide core creates a damage more similar to the BSP projectile, in support of the thesis explained above that the shape of the tip influences the ballistic performance.

3. Conclusions

The Meso-heterogeneous model developed in [1] by the same authors, has been employed in this work to

evaluate the different perforation performances of four types of ammunition of almost identical mass: two AP projectiles, a Ball projectile and a BSP projectile. The results show that the AP projectiles have the lowest ballistic limit, followed by the Ball projectile, while the BSP projectile has the lowest perforation performance. In particular, the ogival ammunition has an impact-residual velocity curve that bends gently, with the best perforation performance by the AP with steel core. The analysis of the morphological features points out that the damage caused by the BSP projectile is the most widespread and severe, with regards to both delamination and deformation of the composite plate. Hence, the AP projectiles have a better perforation performance, but the BSP projectile is able to generate damage on a wider area, also close to its ballistic limit.

References

- [1] L.M. Bresciani, A. Manes, A. Ruggiero, G.Iannitti, M.Giglio. Experimental tests and numerical modelling of ballistic impacts against kevlar29 plain-woven fabrics with epoxy matrix: macro-homogenous and meso-heterogeneous approaches. In revision.
- [2] S.Feli, R.Asgari. Finite element simulation of ceramic/composite armor under ballistic impact. *Composites: Part B*. Vol. 42, pp. 771-780, 2011.
- [3] S.Kulmar, D.S. Gupta, I. Singh, A. Sharma. Behaviour of Kevlar/epoxy composite plates under ballistic Impact. *Journal of Reinforced Plastics and Composites*. 2009. Vol. 29, No. 13, pp. 2048-2064.
- [4] J.H.Ahn, K.H. Nguyen, Y.B. Park, J.H. Kweon, J.H.Choi. A numerical study of the high-velocity impact response of a composite laminate using LS-DYNA. *International Journal of Aeronautical and Space Science*. 2010. Vol.11, pp. 221-226.
- [5] H.L. Gower, D.S. Cronin, A. Plumtree. Ballistic impact response of laminated composite panels. *International Journal of Impact Engineering*. 2008. Vol. 35, pp. 1000-1008.
- [6] M.P. Rao, G. Nilakantan, M. Keefe, B.M Powers, T.A. Bogetti. Global/local modelling of ballistic impact onto woven fabrics. *Journals of composite materials*. 2009. Vol. 43, No. 5, pp 445-467.
- [7] Barauskas, Abraitienė. Computational Analysis of impact of a bullet against the multilayer fabrics in LS-DYNA. *International journal of impact engineering*. 2007. Vol. 34, pp. 1286-1305.
- [8] Bryan A. Cheeseman, Travis A. Bogetti. Ballistic impact into fabric and compliant composite laminates. *Composite structures*. 2003. Vol. 61 pp. 161-173.
- [9] A. Manes, D. Lumassi, L. Giudici, M. Giglio. An experimental-numerical investigation on aluminium tubes subjected to ballistic impact with soft core 7.62 ball projectiles. *Thin-Walled Structures*. 2013. Vol. 73, pp. 68-80.
- [10] A. Manes, F. Serpellini, M. Pagani, M. Saponara; M. Giglio. Perforation and penetration of aluminium target plates by armour piercing bullets. *International Journal of Impact Engineering*. 2014. Vol. 69, pp. 39- 54.
- [11] Naik N.K., Shrirao P., Reddy B.C.K. 2006. Ballistic impact behaviour of woven fabric composites: Formulation. *International Journal of Impact Engineering*. Vol. 32, no. 9, pp. 1521-1552.
- [12] I.M. Daniel. *Engineering mechanics of composite materials*. Oxford University Press.
- [13] C. Herakovich. *Mechanics of Fibrous Composites*. Willey press.
- [14] L.Kollár, G.S.Springer. *Mechanics of composite structures*. Cambridge University Press.
- [15] LS-DYNA® Keyword User's Manual (Version 971 R6.1.0). Livermore Software Technology Corporation, 2012 [16] M.R. Piggott, B. Harris. Compression strength of carbon, glass and Kevlar49 fibre reinforced polyester Resins. *Journal of material science*. 1980. Vol. 15, pp. 2523-2538.
- [17] H.F. Wu, J.R. Yeh. Compressive response of Kevlar epoxy composites: experimental verification. *Journal of material science*. 1992. Vol. 27, pp. 755-760.
- [18] X.S. Zeng, V.B.C. Tan, V.P. Shim. Modelling inter-yarn friction in woven fabric armour. *International Journal for Numerical Methods in Engineering*. 2006. Vol. 66, pp. 1309-1330.
- [19] M.Giglio, A.Gilioli, A.Manes, L.Peroni, M.Scapin. Investigation about the influence of the mechanical properties of lead core and brass jacket of a Nato 7.62 mm ball bullet in numerical simulations of ballistic impacts. *EPJ Web of Conf.*.2012, Vol26.
- [20] L. Peroni, M. Scapin, C. Fichera, A. Manes, M. Giglio. Mechanical properties at high strain-rate of lead core and brass jacket of a Nato 7.62 mm ball bullet. *EPJ Web of Conference*. 2012. Volume 26, 01060
- [21] L. E. Schwer. Impact and Detonation of COMP-B An example using the Ls-Dyna EOS: ignition and growth of reaction in High Explosives. 12th International Ls-Dyna Users Conference, Blast/Impact.
- [22] B. Adams. Simulation of Ballistic impacts on armoured civil vehicles. Master degree thesis at Eindhoven University. 2003.
- [23] J.A. Zukas. *High velocity dynamics*. Wiley press. 1990. pp.1-934.
- [24] A.C.Mitchell, W.J.Nellis. Shock compression of aluminium, copper and tantalum. *J. of Appl. Phys* 1981. V.52, pp. 3363-74.
- [25] R.A. Macdonald, W.M. Macdonald. Thermoynamic properties of fcc metals at high temperatures. *Physical review B*. 1981. Vol. 24, pp. 1715-1724.
- [26] <http://www.nottingham.ac.uk/research/groups/polymer-composites-research-group/research/textile-composites.aspx>